Push–pull hyperbranched molecules. A theoretical study

Estrella Ramos[a], Patricia Guadarrama[a], Gerardo Terán[a] and Serguei Fomine[a]*

The electronic properties of the ground state, unrelaxed and relaxed first excited states of push–pull hyperbranched molecules bearing amino and nitro terminal groups have been studied at BB1K/cc-pvdz//HF/6-31g(d), TD-BB1K/cc-pvdz//HF/6-31g(d) and TD-BB1K/cc-pvdz//CIS/6-31g(d) levels of theory, respectively. It was demonstrated that dendritic architecture of push–pull molecules favours the charge transfer in the excited state compared to linear molecules. The possibility of adopting a plane conformation is an important condition for the charge transfer in an excited state. According to the calculations 1:1 ratio of donor and acceptor groups is another important precondition for the manifestation of strong charge separation in the excited state. In case of excess of nitro groups over the amino, some of the excitations participating in the S0 → S1 transition favour the charge transfer in the excited state in the opposite directions, thus decreasing the charge separation. Copyright © 2008 John Wiley & Sons, Ltd.

Supporting information may be found in the online version of this article.

INTRODUCTION

Donor–acceptor systems[1–4] are very interesting and attractive candidates for applications in molecular electronics, light harvesting and photocatalysis and also find multiple applications in organic photovoltaic cells[5] to convert sunlight into electrical energy.[6] Recently, there has been a great interest in the preparation of photoactive macromolecules on the nanometre scale, and among these, branched molecules have drawn great deal of interest due to their architecture.[7–12] A theoretical study on conjugated phenyl-cored thiophene dendrimers has recently been published describing the optical response and the excited-state properties.[13]

We have developed an efficient synthesis of conjugated dendrons[14] using the Wittig reaction of β,β-dibromostyrens and substituted phenyl acetylenes to afford fully conjugated branched molecules bearing donor and acceptor groups. All oligomers were found to be blue emitters with their emission maxima correlating with the number of the repeating units. It is known that efficient conversion of light into other energy sources requires the formation of charge-separation states that exhibit long lifetimes.[1] Several approaches have been explored in the last few years for this purpose. The most common of them is probably the design of multicomponent systems that separate the photogenerated charges over long distances, either by a cascade of sequential charge migration steps[15] or by the dissociation of the charged components in supramolecular ensembles.[16,17] However, recent studies have demonstrated that there are still many optimizable parameters in simple donor–acceptor models that play a decisive role in the kinetics of charge separation and recombination. Taking the latter into account, another possibility of exploration is the use of branched molecules containing multiple donor and acceptor groups to enhance the charge separation in the excited state.

To gain better understanding of this mechanism of charge separation, we used the quantum chemistry tools to study the electronic properties of the ground and excited states of donor–acceptor hyperbranched molecules and the corresponding linear models.

COMPUTATIONAL DETAILS

All calculations were carried out using Gaussian 03 suite of programs.[18] The theoretical model selection was based on its ability to reproduce the experimental absorption and emission spectra of synthesized molecules. Table 1 shows the experimental and theoretical long wave absorption and emission maxima for various branched conjugated molecules. As seen, the selected model is able to reproduce reasonably well both absorption and emission spectra of selected molecules. Their molecular structures are shown in Scheme 1. Letter **c** in Scheme 1 denotes the linear analogue of the corresponding dendritic molecules denoted as **Na**, where $N = 5$ or 7. When $N = 4$ or 6 the letter **a** corresponds to the molecules with excess of amino groups while **b** means excess of nitro groups. Molecules **1a**, **2a** and **3a** are the reference molecules used for the calibration of the theoretical model.

* Correspondence to: S. Fomine, Instituto de Investigaciones en Materiales, Universidad Nacional Autónoma de México, Apartado Postal 70-360, CU, Coyoacán, México DF 04510, Mexico.
  E-mail: fomine@servidor.unam.mx

a E. Ramos, P. Guadarrama, G. Terán, S. Fomine
  Instituto de Investigaciones en Materiales, Universidad Nacional Autónoma de México, Apartado Postal 70-360, CU, Coyoacán, México DF 04510, Mexico

Table 1. Experimental (λ_{exp}) and theoretical (λ_t) long wave absorption and the corresponding emission ($\lambda_{e\text{-}exp}$ and $\lambda_{e\text{-}t}$) maxima in chloroform, respectively (nm)

Molecule	Λ_{exp}	λ_t	$\lambda_{e\text{-}exp}$	$\lambda_{e\text{-}t}$
1a	377 (Reference 14)	368	443	454
2a	365 (Reference 21)	347	—	—
3a	372	375	—	—
4a	380	394	532	510

First, the extensive conformational searches have been carried out using a mixed torsional/large scale low mode sampling algorithm incorporated in Macromodel 9.0 suite of program using OPLS-AA force field.[19] Each conformational search

included 10 000 iterations. Lowest energy structures obtained were then used as inputs for *ab initio* optimizations without any symmetry restrictions.

The ground state geometry was optimized at HF/6-31G (d) level of theory. Electronic properties of the ground state were calculated using BB1K functional[20] in combination with cc-pvdz basis set. The electronic properties of the unrelaxed S1 state were calculated using the TD-BB1K/cc-pvdz model at HF/6-31G(d) optimized geometry. BB1K functional is available in Gaussian 03 using a combination of keywords BB95 and IOp(3/76 = 0580004200). BB1K-TDDFT excitation energies were shown to be in excellent agreement with experiment for the excitations involving electron transfer.[21]

The geometries of relaxed S1 states were obtained at CIS/ 6-31G(d) level. The electronic properties of the relaxed S1 state were calculated at TD-BB1K/cc-pvdz level using CIS/6-31G(d) optimized geometry. All calculations were carried out in the gas
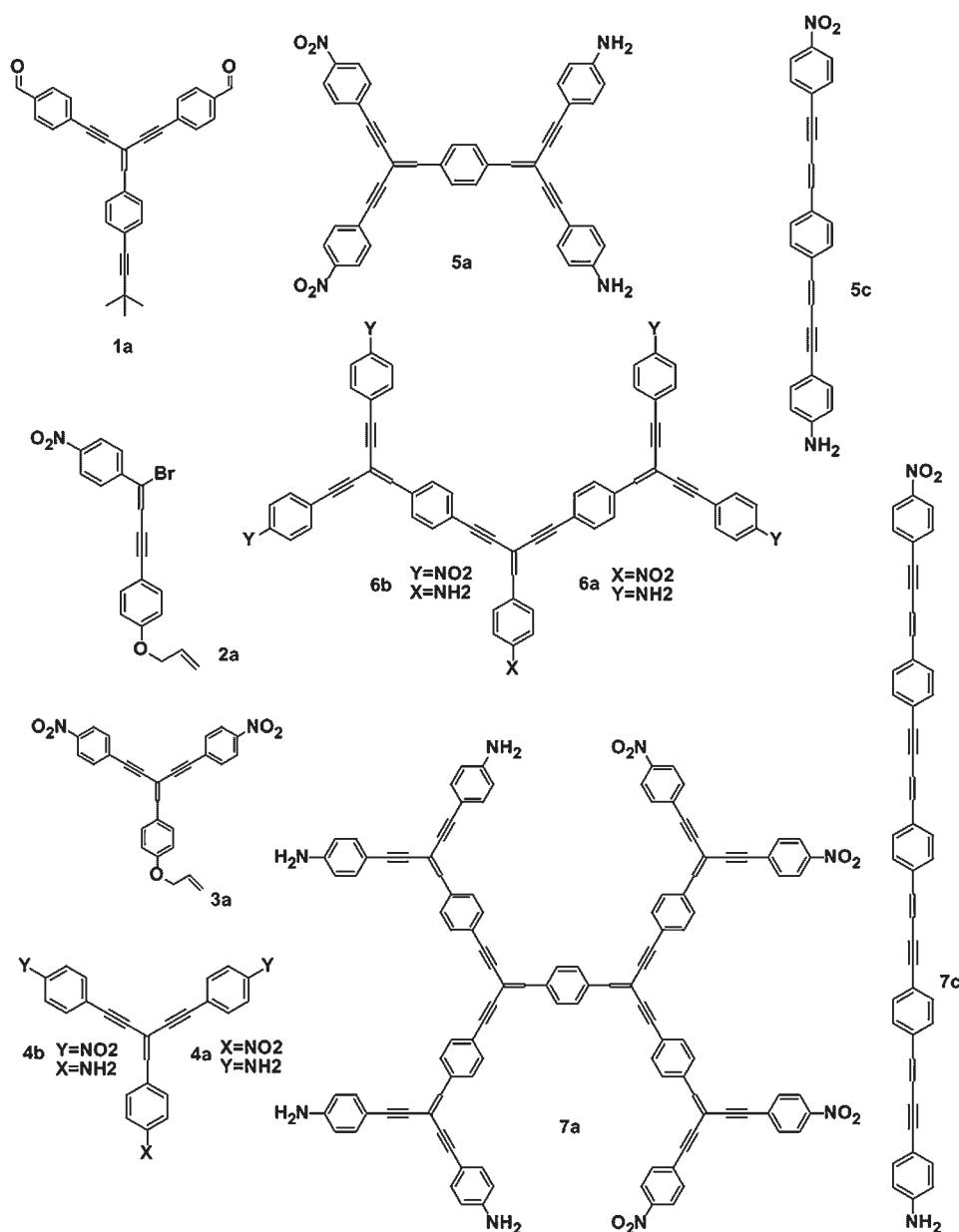
Scheme 1. Structures of studied molecules

phase unless otherwise mentioned. The solvation in chloroform was taken into account using the PCM model incorporated in Gaussian 03 suite of programs.[18] The molecular cavity was specified using the United Atom Topological Model applied on radii optimized for the PBE0/6-31G(d) level of theory (uaks keyword).

EXPERIMENTAL

All reagents were used from Aldrich without any purification. Synthesis of β,β-dibromo-4-nitrostyrene is described in Reference [22]. The visible absorption and emission (excitation at 350 nm) spectra were measured in chloroform using Cary–Eclipse Varian fluorescence spectrometer.

Synthesis of β,β-di(4'-aminophenylethynyl)-4-nitrostyrene(4a)

A mixture of β,β-dibromo-4-nitrostyrene (1.3 mmol), dichlorobis-(triphenylphosphine)palladium (5 mg) and triethylamine (0.2 ml) was stirred in 20 ml of polyethyleneglycol-200 under N_2 atmosphere. 4-ethynylaniline (2.6 mmol) was added dropwise to the solution. The mixture was heated to 80 °C for 8 h.

The reaction mixture was extracted with ether and the raw product was purified by column chromatography on SiO2-ammonia (eluent: hexane:ethylacetate, 1:3) to obtain an orange solid in 60% yield.

^{1}H NMR (CDCl$_3$): 8.2 (d, 2H, *ortho* to NO$_2$), 7.6 (d, 2H, *metha* to NO$_2$), 7.5 (s, 1H, HC=C), 7.3 (d, 2H, *metha* to NH$_2$), 6.6 (d, 2H, *ortho* to NH$_2$).IR (cm^{-1}): 2864 (CH), 3430 (NH), 2357–1946 (C=C), 1600 (C$_{arom}$),1454 (N—O).

RESULTS AND DISCUSSION

Ground state geometry

Figure 1 shows HF/6-31G(d) optimized ground state structures. Nitro and amino groups were selected as strong and typical acceptor and donor groups, respectively to study the properties of branched push–pull molecules. Molecules **5c** and **7c** are the linear analogues of branched molecules of different generations.

As seen, the lowest energy conformers of **5c** and **7c** are quite different. While the global minimum of **7c** is linear, **5c** molecule is bent due to energetically favourable interactions between nitro and amino groups. For **7c**, the bent conformation similar to **5c** is not favoured for steric reasons. To estimate the effect of dendritic architecture on the molecular planarity which is an important characteristic of conjugated systems, the RMS deviation from plane per atom in Å was calculated for all studied molecules and the results are shown in Table 2.

As seen, there are various factors affecting the planarity of conjugated molecules in the ground state. All other things being equal, the planarity of the molecules decreases with branching degree. Thus, as expected, linear molecule **7c** shows RMS deviation from plane 0.00 Å. On the other hand, when comparing **4a**, **4b**, **6a** and **6b** molecules one can notice that while for the molecules **4a,b** nitro groups favour the planarity of dendrons, this is not the case for the next generation **6a,b** molecules. The explanation of this phenomenon is that the electron withdrawing groups favour planarity reducing electron repulsion between aromatics as seen from the comparison of RMS deviation from
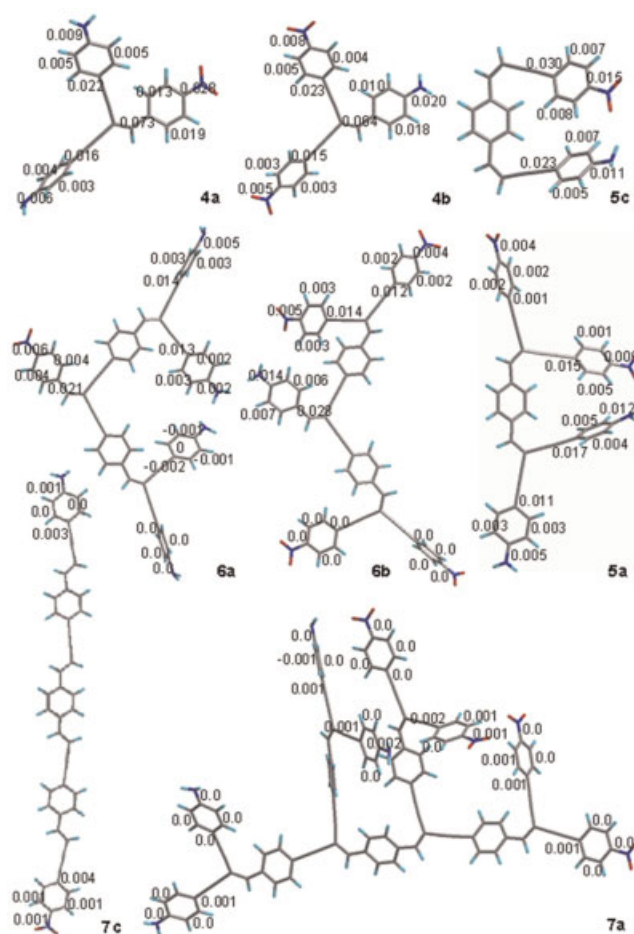

Figure 1. Ground state geometries of studied molecules. The numbers are the differences of the corresponding bond lengths in the ground and excited states in Å

plane for **4a** and **4b** dendrons. The situation is different for **6a** and **6b**, where **6a** is more planar compared to **6b** due to hydrogen bonding between adjacent amino groups as follows from the inspection of their geometry (shortest distance between adjacent NH$_2$ groups is of 2.42 Å). In **4a** this interaction is not possible due to restrictions imposed by the molecular geometry. Therefore, the interactions between terminal groups favour the dendron planarity. This conclusion is also supported comparing the deviations from plane for **6b** and **7a**. Even though **7a** is more branched compared to **6b**, the former molecule is more planar. This is due to interactions between lone pairs of oxygens of nitro group with hydrogen atoms of amino group (Fig. 1).

Excited state geometry

There are two major differences between the geometries of S0 and S1 states of studied molecules (as shown in Supporting Information). The first one is that the RMS deviation from plane is much less for the excited state than for the ground state (Table 2). The second one is the shortening of C—N distances in S1 state (Fig. 1). These changes are the indications of the charge transfer from amino to nitro group occurring in the excited state. According to these results, the electron transfer in the excited state can be represented by resonant structures with formal

Table 2. Dipole moment (μ), (D), topological diameter (D_t) and deviation from plane (Dev) (Å)

| Molecule | μ | | | | | Dev[b] | | |
	$S0_{rel}$	S1	$S1_{rel}$	D_t	$\Delta\mu/D_t$[a]	S0	S1	g/e[c]
4a	8.10	21.38	15.24	14	0.51	32.7(0.71)	10.2 (0.22)	3.23
4b	9.24	19.81	13.44	16	0.26	14.2(0.31)	12.0 (0.26)	1.19
5a	8.37	27.64	20.22	22	0.54	83.6(1.1)	11.6(0.15)	7.33
5c	3.07	19.06	11.12	22	0.37	20.8(0.43)	9.92 (0.21)	2.05
6a	12.41	32.73	28.22	30	0.53	161.5(1.52)	71.8(0.68)	2.23
6b	7.53	19.50	19.22	32	0.37	428.0(4.04)	162 (1.53)	2.64
7a	11.24	25.46	19.08	38	0.21	585.0 (2.98)	468 (2.39)	1.25
7c	9.14	22.12	20.92	38	0.31	0.190 (0.00)	0.19 (0.00)	1

[a] $\Delta\mu = S1_{rel} - S0_{rel}$, $\Delta\mu/D_t$ (D/Å).
[b] RMS deviation from the least-squares plane, with deviation per atom in parenthesis.
[c] Ratio S0/S1 of RMS deviation from plane per atom (deviation per atom).

double bonds between the aromatic rings and amino and nitro groups, respectively, as shown in Fig. 2. The planarization and C—N distances shortening in the excited state although confirming the electron transfer from amino to nitro groups in excited state cannot be taken as a measure of this transfer because both these parameters depend on steric factors and the electron count in the molecules. However, several conclusions can be made comparing similar molecules. Thus, as seen from Fig. 1 differences in C—NO_2 and C—NH_2 distancesbetween ground and excited states are significantly larger for branched molecules **4a** and **4b**, respectively, compared to linear analogue **5c** demonstrating dendritic effect on the electron transfer in the excited state. Similar observation can be made for the molecules **6a**, **6b** and **7c**. As seen from Fig. 1 differences in C—NO_2 and C—NH_2 distance between S0 and S1 states for **6a** and **6b** are of 0.006 and 0.014 Å, while for linear **7a** molecule these differences are of 0.001 and 0.002 Å, respectively.

Excitation, emission energies and dipole moments

Table 3 shows the calculated S0 → S1 transition energies. As seen from Table 3 the vertical excitation energies of the dendrimer and the corresponding linear analogues decrease with the number of aromatic rings in the molecule and do not depend on the molecular architecture. Thus, NO_2 group causes larger red shift compared to NH_2 (**4a**, **4b** and **6a**, **6b**) since NO_2 introduces larger conjugation compared to NH_2. The situation changes for
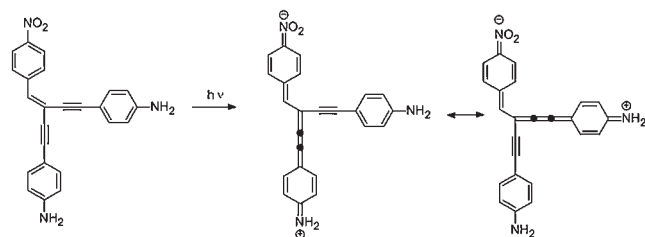

Figure 2. Resonant structures representing electron transfer in excited state

emission energies where no apparent correlation between the emission energy and the effective conjugation length (the number of aromatic rings) is observed as seen from Table 3.

The lowest emission energy is found for **5a** followed by **7a**. These molecules have multiple donor and acceptor groups, resulting in better stabilization of CT excited state. **5a** has two nitro and two amino groups, while **7a** has four nitro and four amino groups. As seen from Table 3 these molecules show the largest Stock shifts, supporting this hypothesis. Table 4 shows the total energies for excited states, as well as the relaxation energies. The direct comparison of the energy difference between relaxed and unrelaxed S1 states (Table 4) shows that the largest relaxation energy is for **5a** closely followed by **7a**. Thus, the best stabilization of CT excited state occurs for the dendritic structures with equal number of donor and acceptor groups. Steric factors play an important role since the excessively branched molecule **7a** is unable to adopt the geometry plane enough to stabilize the S1 state to the same extent as **5a** does, as seen from the comparison of RMS deviation from plane data for S0 and S1 states (Table 2). The ratio g/e is 7.33, the largest for **5a** dendrimer while it is 1.25, for **7a** dendrimer reflecting steric hindrances in this molecule.

The charge transfer degree on photoexcitation can be estimated by the comparison of the dipole moments in S0 and S1 states (as shown in Table 2). However, the direct comparison of the dipole moments is not totally correct due to the size differences between the molecules. To compare the charge transfer in the excited states we used $\Delta\mu/D_t$ index where $\Delta\mu$ is the difference of the dipole moments between the ground and excited states of the same molecule and D_t is the topological diameter of the system i.e. the maximum topological distance in the molecule. Table 2 shows the dipole moments in the ground and excited states as well as $\Delta\mu/D_t$ indexes. As seen the dipole moments in the ground state depend mostly on the geometry of global minimum conformation. Thus, the small dipole moment of **5c** is due to its bent conformation and **4b** has larger dipole moment than **4a** in the ground state. The situation changes for the next generation dendrons (**6a** and **6b**) where **6a** has larger dipole moment due to conformational differences (as shown in Supporting Information). As seen from Table 2 the excitation from

12

www.interscience.wiley.com/journal/poc

Copyright © 2008 John Wiley & Sons, Ltd.

J. Phys. Org. Chem. **2009**, 22 9–16

Table 3. Calculated orbitals involved in S0→S1 excitation and the corresponding expansion coefficients (C_i), Stock shifts (nm), long wave (nm) absorption and emission (in brackets) maxima of studied molecules

Molecule	S0 → S1	C_i	Stocks shift	λ
4a	HOMO → LUMO	0.65	99.4	371.25(470.69)
4b	HOMO → LUMO	0.65	93.0	371.72(464.75)
5a	HOMO − 2 → LUMO	−0.22	162.6	412.52(575.09)
	HOMO → LUMO	0.60		
	HOMO → LUMO + 2	−0.18		
5c	HOMO → LUMO	0.68	118.0	390.75(508.74)
6a	HOMO − 4 → LUMO	0.14	89.9	405.33(495.22)
	HOMO → LUMO	0.61		
	HOMO → LUMO + 1	−0.18		
	HOMO → LUMO + 2	0.16		
6b	HOMO − 1 → LUMO	−0.11	107.1	409.14(516.19)
	HOMO − 1 → LUMO + 1	0.13		
	HOMO → LUMO	0.61		
	HOMO → LUMO + 4	0.19		
7a	HOMO − 3 → LUMO	−0.29	153.2	434.09(587.30)
	HOMO − 3 → LUMO + 3	0.12		
	HOMO − 2 → LUMO	−0.19		
	HOMO − 1 → LUMO	0.12		
	HOMO → LUMO	0.37		
	HOMO → LUMO + 1	0.10		
	HOMO → LUMO + 3	−0.24		
	HOMO → LUMO + 2	−0.11		
	HOMO → LUMO + 4	0.14		
	HOMO → LUMO + 6	0.13		
7c	HOMO − 2 → LUMO	−0.11	73.6	402.06(475.68)
	HOMO − 2 → LUMO + 1	−0.10		
	HOMO − 1 → LUMO	0.36		
	HOMO − 1 → LUMO + 1	−0.16		
	HOMO − 1 → LUMO + 2	0.11		
	HOMO → LUMO	−0.34		
	HOMO → LUMO + 1	0.35		
	HOMO → LUMO + 2	0.12		

S0 to S1 state results in significant increase of dipole moment indicating the charge transfer along the molecule. As follows from TD calculations in all cases the most important contribution into S0 → S1 transition represents HOMO–LUMO excitation.

Table 4. Total energies of unrelaxed S1 states and the corresponding relaxation energies in a.u. and eV, respectively

Molecule	S1	E_r[a]
4a	−1238.676305	0.484
4b	−1387.780282	0.411
5a	−2134.667903	0.835
5c	−1260.714612	0.676
6a	−2732.439740	0.527
6b	−3179.745945	0.619
7a	−5420.385729	0.838
7c	−2029.627397	0.509

[a] Relaxation energy defined as (S1 − S1$_{rel}$).

Figure 3 shows the molecular orbitals contributing to the excitation with C_i expansion coefficients of at least 0.1. The corresponding coefficients are shown in Table 3. As seen, for the molecules **4a**, **4b** and **5c** the only important excitation is HOMO–LUMO one.

The number of excitations contributing to S0 → S1 transition increases with molecular size, however, in all cases except for **7c** HOMO–LUMO excitation prevails. As seen from MO plots (Fig. 3a and b) the interpretation of S0 → S1 transition for **4a**, **4b** and **5c** is rather straightforward meaning the electron transfer from the 'donor' moiety to the 'acceptor' moiety. In the case of **4a** and **4b**, the 'donor' and the 'acceptor' moiety include two amino and two nitro groups, respectively, while in the case of **5c** the 'donor' and 'acceptor' moiety involve one amino and one nitro group, respectively. As a consequence **4a** and **4b** excited state geometries show greater contribution from quinoid structure (Fig. 2) to the geometry of their excited states compared to linear **5c** (Fig. 3b). The introduction of two amino and two nitro groups into molecular structure (**5a**) further improves the charge transfer in the excited state as seen from Fig. 3b. HOMO includes atomic orbitals of two NH_2 groups and LUMO includes the corresponding
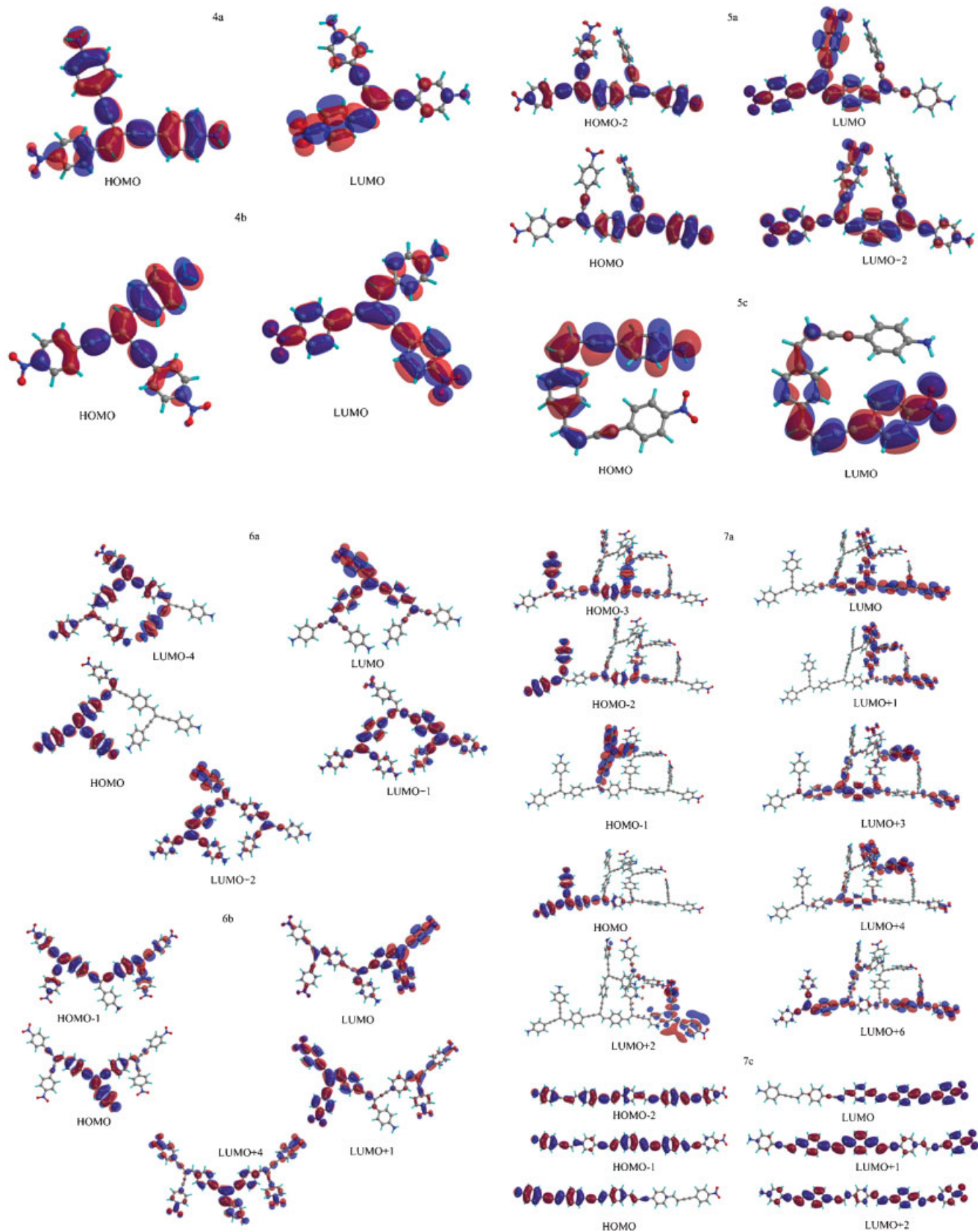
Figure 3. (a) Molecular orbitals involved in S0 → S1 transition for **4a** and **4b** molecules; (b) molecular orbitals involved in S0 → S1 transition for **5a** and **5c** molecules; (c) molecular orbitals involved in S0 → S1 transition for **6a** and **6b** molecules; (d) molecular orbitals involved in S0 → S1 transition for **7a** and **7c** molecules

orbitals of two nitro groups. In fact, **5a** has the highest $\Delta\mu/D_t$ index for the relaxed S1 state of all molecules (0.54), indicative of the best charge transfer on excitation. Unlike **4a**, in the case of **6a** the most important HOMO–LUMO excitation for S0 → S1 transition involves only half of all amino groups available in molecule. Another excitation contributing to the charge transfer is HOMO − 4 → LUMO (Fig. 3c) with smaller coefficient (as shown in Table 3). However, as seen from Fig. 3c one of the four NH$_2$ groups in **6a** does not participate in the charge transfer. Similar situation holds for **6b** where only HOMO → LUMO excitation contributes to the charge transfer. Three other excitations do not contribute significantly to the electron transfer from amino to nitro groups as seen from Fig. 3c. $\Delta\mu/D_t$ index is in line with the orbital analysis of S0 → S1 excitation; for **6a** $\Delta\mu/D_t$ is less than for **5a** and for **6b** $\Delta\mu/D_t$ is less than for **6b** (as shown in Table 2). As can be seen from Table 3 and Fig. 3d all the excitations involved in S0 → S1 transition in **7a** contribute to the charge transfer from the 'donor' to 'acceptor' moiety. However, the $\Delta\mu/D_t$ index (Table 2) calculated for the relaxed S1 state is the lowest of all studied molecules. This observation agrees with the fact that **7a** shows the largest deviation from plane in both ground and excited states and the lowest ratio out of all molecules except for **7c** since **7c** is essentially plane even in the ground state. In fact, the $\Delta\mu/D_t$ index is higher for **7c** compared to **7a** due to the plane geometry of the former. As seen from Fig. 3c and Table 3 the only excitation contributing to the charge transfer in the excited state in **7c** is HOMO–LUMO transition.
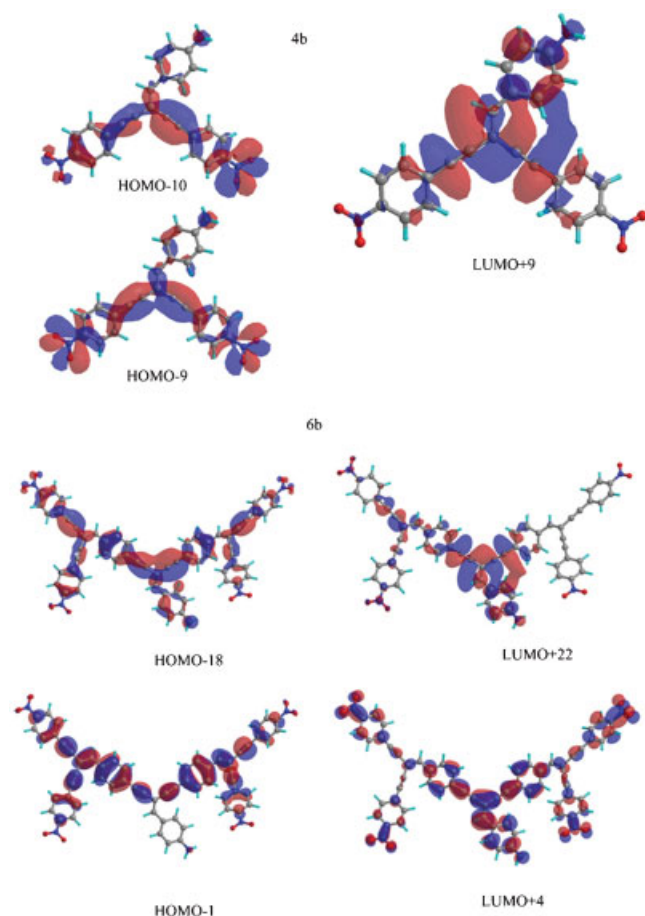
As can be seen from Table 2 the dipole moments of dendrons **4b** and **6b** in the ground state are larger than those of **4a** and **4b**, however, in the excited state the situation reverses; **4a** and **6a** have larger dipole moments than **4b** and **6b**. Therefore, $\Delta\mu/D_t$ index is higher for **4a** and **6a** compared to **4b** and **6b** (Table 2) evidencing better charge transfer in the excited state for dendrimers with multiple amino groups compared to multiple nitro groups. This difference between nitro and amino groups can be understood analysing excitations contributing to S0 → S1 transition in different molecules. All contributions with expansion coefficients greater than 0.01 were analysed for molecules **4a**, **4b**, **6a** and **6b**. While for dendrons **4a** and **6a** all excitations involved in S0 → S1 transition implied the charge transfer from 'donor' to 'acceptor' moieties in case of **4b** and **6b** excitations involving MOs shown in Fig. 4 favours the charge transfer in the opposite direction, thus reducing the dipole moment in excited state compared to **4a** and **6b** dendrons.

CONCLUSIONS

Calculations showed that dendritic structure of push–pull molecules favours the charge transfer in the excited state. Thus, the contribution to the excited state geometry from zwitter ionic quinoid structure is larger for dendritic **4a** and **4b** molecules (Fig. 2) compared to linear **5c**. An important condition for the manifestation of dendritic effect is the possibility for the molecule to adopt planar conformation in excited state. Thus, the charge transfer in the excited state is higher for **4a**, **4b** and **5a** compared to **6a**, **6b** and **7a** due to steric hindrances to adopt plane conformation for the latter. According to the analysis of the dipole moments in the ground and excited states, the most efficient charge transfer occurs in **5a** dendron evidencing that 1:1 ratio of donor to acceptor group is another important precondition for the molecule to show strong charge transfer in the excited state. All other things being equal, the excess of amino groups is preferable to the excess of nitro groups for studied dendrimers to manifest strong charge transfer in the excited state due to the fact that in molecules **4b** and **6b** some of the excitations contributing to S0 → S1 transition favour the charge transfer in the opposite direction.

SUPPORTING INFORMATION

Cartesian coordinates of optimized geometries of studied molecules are available in the supplementary material.

Figure 4. Some of the molecular orbitals involved in S0 → S1 transition for molecules **4b** and **6b**

REFERENCES

[1] Eds.: V., Balzani, P. Piotrowiak, , *Electron Transfer in Chemistry*, Vols. 1-5, Wiley-VCH, New York, NY, **2001**.
[2] M. R. Wasielewski, *Chem. Rev.* **1992**, *92*, 435.
[3] M. N. Paddon-Row, *Electron and Energy Transfer, In Stimulating Concepts in Chemistry* (Eds.: F., Vögtle, J., Stoddart, M. Shibasaki), Wiley-VCH, New York, NY, **2000**, pp 267–291.

[4] J. Cremer, E. Mena-Osteritz, Neil, G. Pschierer, K. Müllen, P. Bäuerle, *Org. Biomol. Chem.* **2005**, *3*, 985.
[5] B. O'Regan, M. Grätzel, *Nature* **1991**, *353*, 737.
[6] A. M. Ramos, S. C. J. Meskers, P. A. van Hal, J. Knol, J. C. Hummelen, R. A. J. Janssen, *J. Phys. Chem. A* **2003**, *107*, 9269.
[7] T. H. Kwon, M. K. Kim, J. Kwon, D. Y. Shin, S. J. Park, C. L. Lee, J. J. Kim, J. I. Hong, *Chem. Mater.* **2007**, *19*, 3673.
[8] A. Petrella, J. Cremer, L. De Cola, P. Bäuerle, R. M. Williams, *J. Phys. Chem. A* **2005**, *109*, 11687.
[9] V. Parra, T. Del Caño, M. J. Gómez-Escalonilla, F. Langa, M. L. Rodrı́guez-Méndez, J. A. De Saja, *Synth. Met.* **2005**, *148*, 47.
[10] S.-C. Lo, P. L. Burn, *Chem. Rev.* **2007**, *107*, 1097.
[11] J. Qiao, C. Yang, Q. He, F. Bai, Y. Li, *J. Appl. Polym. Sci.* **2004**, *92*, 1459.
[12] C.-Q. Ma, E. Mena-Osteritz, T. Debaerdemaeker, M. M. Wienk, R. A. Janssen, P. Bäuerle, *Angew. Chem. Int. Ed.* **2007**, *46*, 1679.
[13] M. E. Köse, W. J. Mitchell, N. Kopidakis, C. H. Chang, S. E. Shaheen, K. Kim, G. Rumbles, *J. Am. Chem. Soc.* **2007**, *129*, 14257.
[14] L. Fomina, P. Guadarrama, S. Fomine, R. Salcedo, T. Ogawa, *Polymer* **1998**, *39*, 2629.
[15] D. Gust, T. A. Moore, A. L. Moore, *Acc. Chem. Res.* **2001**, *34*, 40.
[16] D. M. Guldi, N. Martín, *J. Mater. Chem.* **2002**, *12*, 1978.
[17] L. Sánchez, N. Martín, D. M. Guldi, *Angew. Chem. Int. Ed.* **2005**, *44*, 5374.
[18] M. J. Frisch, G. W. Trucks, H. B. Schlegel, G. E. Scuseria, M. A. Robb, J. R. Cheeseman, V. G. Zakrzewski, A. Montgomery, R. E. Stratmann, Jr, J. C. Burant, S. Dapprich, J. M. Millam, A. D. Daniels, K. N. Kudin, M. C. Strain, O. Farkas, J. Tomasi, V. Barone, M. Cossi, R. Cammi, B. Mennucci, C. Pomelli, C. Adamo, S. Clifford, J. Ochterski, G. A. Petersson, P. Y. Ayala, Q. Cui, K. Morokuma, D. K. Malick, A. D. Rabuck, K. Raghavachari, J. B. Foresman, J. Cioslowski, J. V. Ortiz, A. G. Baboul, B. B. Stefanov, G. Liu, A. Liashenko, P. Piskorz, I. Komaromi, R. Gomperts, R. L. Martin, D. J. Fox, T. Keith, M. A. Al-Laham, C. Y. Peng, A. Nanayakkara, M. Challacombe, P. M. W. Gill, B. Johnson, W. Chen, M. W. Wong, J. L. Andres, C. Gonzalez, M. Head-Gordon, E. S. Replogle, J. A. Pople, Gaussian, Inc; Wallingford CT, **2004**.
[19] MacroModel 9.0, supplied by Schrödinger, Portland, OR.
[20] Y. Zhao, B. J. Lynch, D. G. Truhlar, *J. Phys. Chem. A.* **2004**, *108*, 2715.
[21] J. To, A. Sokol, S. French, N. Kaltsoyannis, R. Catlow, *J. Chem. Phys.* **2005**, *122*, 144704.
[22] S. Fomine, L. Fomina, R. Jiménez, E. Popova, T. Ogawa, *Mendeleev Commun.* **1998**, *8*, 117.